Dead-end filtration of yeast suspensions: Correlating specific resistance and flux data using artificial neural networks

Jenny Ní Mhurchú and Greg Foley

School of Biotechnology and National Institute for Cellular Biotechnology, Dublin City University, Dublin 9, Ireland

Abstract

The specific cake resistance in dead-end filtration is a complex function of suspension properties and operating conditions. In this study, the specific resistance of resuspended dried bakers yeast suspensions was measured in a series of 150 experiments covering a range of pressures, cell concentrations, pHs, ionic strengths and membrane resistances. The specific resistance was found to increase linearly with pressure and exhibited a complex dependence on pH and ionic strength. The specific resistance data were correlated using an artificial neural network containing a single hidden layer with nine neurons employing the sigmoidal activation function. The network was trained with 104 training points, 13 validation points and 33 test points. Excellent agreement was obtained between the neural network and the test data with average errors of less than 10%. In addition, a network was trained for prediction of the filtrate flux directly from the system inputs and this approach is easily extended to crossflow filtration by adding inputs such as the crossflow velocity and channel height. An attempt was made to interpret the network weights for both the specific resistance and flux networks. The effective contribution of each input to the system output was computed in each case and showed trends that were as expected. Although network weights, and consequently the computed effect of each parameter, is different each time a network is changed (depending on the initial weights used in the training process), the variation was low enough for information contained in the network to be interpreted in a meaningful way.

Keywords: Dead-end filtration; Specific cake resistance; Artificial neural network; Bakers yeast

Nomenclature

a	constant in equation [5]
A	membrane area (m^2)
b	constant in equation [5]
c	mass of solids per unit volume of filtrate (kg/m^3)
J	filtrate flux (m/s)
m	mass of cake per unit membrane area (kg/m^2)
MSE	maximum squared error
n_h	number of neurons in hidden layer
n_v	number of input variables
O_j	absolute value of the weight from the jth neuron in hidden layer
ΔP	applied pressure (N/m^2)
ΔP_c	cake pressure drop (N/m^2)
R_c	cake resistance (m^{-1})
R_m	membrane resistance (m^{-1})
R_T	total resistance to flow (m^{-1})
t	time (s)
$\underline{v}$	relative effect of input variable
V	filtrate volume (m^3)
$\underline{w_{kj}}$	absolute value of weight from kth input to the jth hidden neuron
$\underline{w_{vj}}$	absolute value of weight from the input of interest to the jth hidden neuron
x_i	data point to be normalised
x_i'	normalised data value
x_{min}	minimum value of data point
x_{max}	maximum value of data point

Greek letters

α	specific cake resistance (m/kg)
μ	filtrate viscosity ($N\ s/m^2$)

1. Introduction

Membrane filtration is frequently used for the separation of solids such as colloids and microbial cells from liquids. Applications range from treatment of industrial wastewater to purification of drinking water, to dairy processing, to the removal of macromolecules (proteins, polyphenols, polysaccharides, etc.) from beer and wine. Microfiltration in particular is an efficient technique for separating particles ranging from 0.1 μm up to a few microns in size from a liquid medium [1]. It can be conducted using two distinct modes of operation referred to as dead-end and crossflow microfiltration. In the dead-end configuration, the feed suspension flows perpendicular to the membrane surface, whereas in crossflow systems, the suspension flow is tangential to the membrane.

Filtration performance is usually expressed in terms of the filtrate flux, *J*, defined as the filtrate flowrate per unit membrane area. This is typically related to the applied pressure through the expression

$$J = \frac{\Delta P}{\mu\left(R_m + \alpha m\right)} \tag{1}$$

where *J* is the filtrate flux, Δ*P* the applied (trans-membrane) pressure, μ the filtrate viscosity, R_m the membrane resistance, α the specific cake resistance and *m* is the cake mass per unit membrane area. In dead-end filtration, *m* can be related to the filtrate volume, *V*, by the expression

$$m = \frac{cV}{A} \tag{2}$$

where *A* is the membrane area and *c* is the mass of solid particles per unit volume of filtrate. The specific cake resistance can be measured (or process performance calculated) from the well-known expression, derived using Eqs. (1) and (2) and valid for constant pressure filtration [2], namely

$$\frac{t}{V} = \frac{\mu R_m}{A\Delta P} + \frac{\alpha\mu c}{2A^2\Delta P}V \tag{3}$$

In membrane filtration operations, the specific cake resistance can be considered to be a measure of the 'filterability' of suspensions as its value determines to a large extent the efficiency of a process. However, while filtration equations are simple in form, much complexity is concealed because the specific resistance is dependent on many other variables. Traditionally, the main factor assumed to affect the specific resistance is the pressure drop across the filter cake, ΔP_c, where this quantity is defined by the expression

$$\Delta P_c = \Delta P - \mu R_m J \tag{4}$$

Although α is technically dependent on cake pressure drop, most authors correlate dead-end specific resistance data in terms of the total applied pressure, Δ*P*, an approach that that is reasonable as long as the cake resistance is dominant throughout the filtration. The equations used to correlate specific resistance data are varied but most authors use the classic power-law equation [3], [4] and [5] or, in some cases (especially for microbial suspensions), a linear relationship between specific resistance and pressure is employed [6], [7] and [8].

The specific cake resistance is dependent on many parameters other than pressure. Ionic strength and pH are well known to influence specific resistance in a complex manner that is very system specific [9], [10] and [11]. In addition to the effects of pH and ionic strength, microbial filtration is complicated by subtleties that arise due to the biological nature of the suspensions. Hodgson et al. [12] demonstrated the importance of cell surface properties on filtration behaviour. Very often these properties are affected by, and related to, conditions such as the type of growth medium used to produce the cells [13] and [14], the stage of the growth cycle at which the cells are harvested for filtration and the possibility of cell aging between halting the fermentation and performing the filtration [15] and [16].

As well as causing changes in cell surface properties, medium components may also provide additional resistance to flow. Solid medium components may cause cake clogging [17] while concentration polarisation of soluble components may also be significant if solute rejection occurs [18]. Both of these phenomena may increase the effective specific cake resistance.

Further complications have been suggested by Mota et al. [19], who have found evidence that the specific resistance of yeast suspensions increases with increasing suspension concentration, a finding that is supported in recent work on the ultrafiltration of silica suspensions [20]. These findings are atypical as most authors would consider the specific resistance to be independent of concentration.

Given the number of factors affecting the specific cake resistance, prediction of this parameter becomes problematic. While conventional non-linear regression approaches could be used to derive experimental correlations, the complexity of the problem, especially the dependence of specific resistance on pH and ionic strength, makes such an approach difficult and likely to lead to very complex and unwieldy empirical equations. In this context, artificial neural networks (ANNs) may provide a promising avenue of research. The aim of an approach based on ANNs is not unlike that of conventional non-linear regression in that experimental data can be used to develop computational algorithms that will allow a given quantity to be predicted for any set of process variables within the range of the original experimental data [21]. While the network architecture must be chosen after some numerical experimentation, no assumptions about the functional relationship between the independent (input) variables and the dependent variables (output) are required. Furthermore, even quite simple network architectures can reproduce highly complex non-linear behaviour. Recently, ANNs have been employed in a number of studies to model the flux dynamics of crossflow membrane filtration processes, including microfiltration [22], [23], [24], [25], [26] and [27], but have not yet been employed for dead-end microfiltration of particulate or cellular suspensions.

In the study reported here, we have measured the specific resistance and steady flux through cakes formed by bakers yeast suspensions over a range pressures, pHs, ionic strengths, cell concentrations and membrane resistances. ANNs are constructed, trained and validated and found to perform well in the correlation and prediction of specific resistance and filtrate flux. Furthermore, an attempt is made to interpret the relative effects of the network inputs on the network output.

2. Materials and methods

2.1. Yeast suspensions

Experiments were conducted with suspensions of dried 'Fermipan' bakers yeast (DSM Bakeries, Holland) resuspended in distilled water and prepared freshly before use. Suspensions were washed twice with a 0.5 M NaOH solution and then three times with distilled water. The washing step involved suspension of 1.5 g of cells in 15 mL of either NaOH or distilled water, followed by centrifugation for 3 min at 58.33 Hz (3500 rpm), and the supernatant removed. Cells were washed in caustic solution because washing in pure water alone resulted in protein that had leached from the cells remaining in the suspension. It is well established that proteins can cause fouling of microfiltration membranes and the presence of this protein would have affected the specific cake resistance measurements. The dry mass of cells after the washing steps was found to be 50% of the unwashed dry mass and it is this dry mass concentration that is reported throughout the paper. The pH of each solution was adjusted to the desired value by adding either 0.5 M HCl or 0.5 M NaOH. The salt concentration (and therefore the ionic strength) was adjusted by adding NaCl.

2.2. Membranes

Experiments were performed using the following hydrophilic polyethersulphone membrane discs (47 mm diameter): (i) a Supor®-450 membrane filter from Pall Corporation with a nominal pore size of 0.45 μm and a thickness of 140 μm, and (ii) a Supor®-200 membrane filter from the same supplier with a nominal pore size of 0.2 μm and a thickness of 145 μm. The 0.45 μm membrane had a mean resistance to flow of 1.78×10^{10} m^{-1}, and the 0.2 μm membrane had a mean resistance to flow of 3.81×10^{10} m^{-1}. Slight variability (in the order of 10–15%) in the membrane resistances was noted. A clean membrane was used for each run, and the membrane resistance was experimentally determined before each run. The membranes were supported in the filtration cell with circumferential supports of width 1 mm and the effective filtration area was 1.59×10^{-3} m^2.

2.3. Filter cell

Microfiltration experiments were carried out using a 150 mL, 47 mm diameter stainless steel dead-end filtration cell from Pall Corporation. The cell was pressurised using compressed air and the pressure controlled using a regulator. All experiments were carried out at room temperature. Fresh yeast suspension and a new membrane were loaded into the apparatus for each experiment. The filtrate was collected in a reservoir placed on an electronic balance (Mettler Toledo BS3001) interfaced to a computer using Winwedge® software (TAL Technologies Inc., PA, USA) to collect and record time and filtrate mass data at 1 s intervals. After each run, the apparatus was thoroughly cleaned using Teepol detergent, followed by a rinse of distilled water.

2.4. Filtration method

The membrane resistances were determined by measuring the filtrate flux of distilled water through the membrane at a fixed pressure and applying Eq. (1) with $m = 0$. The steady-state method [3] was employed to determine the specific resistance of the filter cake. In this method, a given volume of yeast suspension (typically 100 mL), containing a known dry mass of yeast, was filtered at a pressure of 0.2×10^5 Pa (0.2 bar). Once the initial (dynamic) filtration was complete, the pressure was released. The

filtrate was carefully returned to the filtration module, ensuring that the cake of cells was not disturbed. The cell was re-pressurised to the pressure employed to form the filter cake (0.2×10^5 Pa (0.2 bar)) and filtration recommenced. The filtrate flux was allowed to reach steady-state before the transmembrane pressure was incremented to the next pressure, and recorded at five different pressures between 0.2 and 2×10^5 Pa (0.2 and 2 bar). The filtrate mass was monitored continuously throughout the experiment and the steady-state flux was determined from this measurement for each pressure. The specific resistance was then calculated by applying Eq. (1). It should be noted that it is generally found that the specific resistance of a microbial cake at a given pressure is independent of whether or not the cake has been exposed previously to different pressures [28] and hence the approach of incrementing the pressures in the way described above is valid.

The membrane was examined for evidence of irreversible fouling after each experiment. This was achieved by washing the membrane with distilled water and then measuring the flux of distilled water through the washed membrane. Although there was some evidence of membrane fouling, the membrane resistance before and after filtration was of the order of 10^{10} m^{-1}, whereas the cake resistance ranges between 10^{12} and 10^{13} m^{-1}. Therefore, the increase in membrane resistance due to fouling does not affect the filtration characteristics and the cake resistance is the limiting resistance.

2.5. Experimental design

The experimental data in this work were collected for the purpose of attempting to model and predict the specific resistance and filtrate flux in dead-end microfiltration using an artificial neural network. The process parameters that were identified as being important in determining the specific cake resistance and filtrate flux were the pressure, yeast concentration, pH, salt concentration and membrane resistance. In the case of the specific resistance, the expectation would normally be that the effect of concentration should be negligible despite recent findings to the contrary [19] and [20]. Similarly one would expect the effect of membrane resistance on both the specific resistance and the flux to be small. Nevertheless, the effects of both cell concentration and membrane resistance were examined, in order to ascertain whether the predictions of the Garson Equation (described in Section 3.5) agree with these findings.

The experimental population was devised using a range of possible combinations of the process parameters that were deemed of importance in the dead-end filtration of the yeast suspensions employed in this study. These were arbitrarily set to the values outlined in Table 1. All of the possible combinations of the values of the parameters outlined in Table 1 were numbered and using a random number generator, 30 experiments were chosen at random. The reason for choosing a random sample of experiments is to illustrate the applicability of the neural network approach to a process in which interactions between parameters are not necessarily understood. This lack of understanding would make impossible the use of a partial factorial design, for example. Choosing the experiments randomly needs no prior knowledge of the effect of the process parameters or their interactions on the experimental outcome.

Table 1: Process Parameters

Yeast concentration (g/L)	pH	NaCl concentration (g/L)	R_m (m^{-1})	ΔP ($\times 10^5$ Pa (bar))
3	2	0	1.78×10^{10}	0.2
5	3	1	3.81×10^{10}	0.5
7	4	2		1.0
9	5	3		1.5
11	6	4		2.0
13	7	5		
15	8	6		

Each combination of process parameters was performed at five different pressures, so a sample of 150 experiments was thus performed from all of the possible combinations of the process parameters. The specific resistance and steady-state flux were experimentally determined for each parameter combination selected.

2.6. Artificial neural networks

The principles of artificial neural networks and their application to membrane processes have been described in detail previously in the studies mentioned in Section 1 and here we only give the key features of our implementation of this approach. A feed-forward ANN employing the sigmoid transfer function and the Levenberg-Marquardt algorithm for training was constructed with the MATLAB 7.0 Neural Networks Toolbox (The MathWorks Ltd., UK). All network weights were assigned random initial values in the range (−0.1, +0.1), training was conducted in batch mode and the training rate was set at the Matlab default value. Input data were normalised according to the following expression, used by Fu et al. [21]

$$x_i^* = a\frac{x_i - x_{\min}}{x_{\max} - x_{\min}} + b \quad (5)$$

Where x_i* is the normalised value, x_i the original data point, x_{max} and x_{min}, respectively, the maximum and minimum values for x, and a and b are the positive constants allowing the limits of the interval for the scaled values to be fixed. In this paper, a and b are set as 0.6 and 0.2, thus the range of the data after normalisation is (0.2, 0.8). The scale of the sigmoid transfer function is (0, 1), so training the network in the range 0.2–0.8 allows a margin for extrapolation outside the range of the training data.

The data in this study were divided into three sub-sets: a training set, a validation set and a test set as described previously [29] and [30]. Using a technique known as cross-validation, the validation set prevents over-training of the network by stopping training early once the maximum squared error (MSE) in the validation set begins to increase. The number of training points was chosen arbitrarily to be 104 and training points were selected to ensure that extreme values of the output (specific cake resistance) were included in the training set, as is clear from Fig. 1. The number of validation points was 13 and the number of test points was 33. It has been shown by Amari et al. [31] that the number of data points used for cross-validation should be very small compared to the number of training points. Reduction in the number of training data points reduced the accuracy of the final network. Table 2 provides a

summary of all the experimental conditions employed and shows which experiments were used for training, validation and testing.

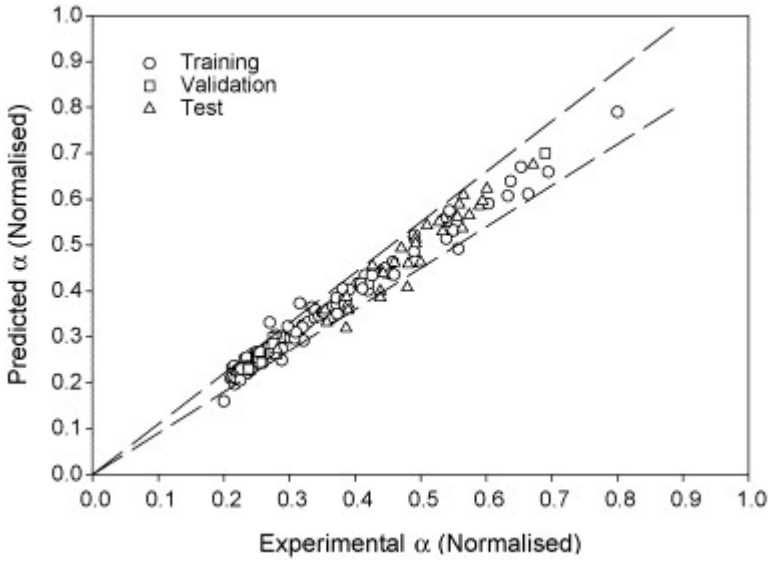

Figure 1: Fit of 5-9-1 network to specific resistance data. Dashed lines denote ± 10% variation from the y=x line

Table 2: Experimental combinations and choice of training, validation and testing points

Yeast concentration (g/L)	pH	Salt concentration (g/L)	Pore size (µm)	Training (T), validation (V), test (X)[a]
3	2	5	0.2	T, T, T, T, T
3	2	2	0.2	T, V, T, T, T
3	7	2	0.45	T, V, T, T, T
3	9	4	0.2	T, X, T, T, X
5	4	0	0.45	T, T, T, X, X
5	5	5	0.45	T, V, T, T, T
5	9	4	0.2	T, X, V, X, X
7	2	1	0.45	T, V, T, T, T
7	2	5	0.45	T, T, T, T, X
7	4	0	0.2	T, T, T, T, X
7	4	1	0.45	T, T, X, T, T
7	8	2	0.2	T, T, X, T, X
7	8	6	0.2	T, T, T, X, T
7	9	4	0.2	T, X, T, X, X
9	5	3	0.2	T, T, T, T, V
9	5	4	0.2	T, T, T, X, T
9	9	0	0.2	V, T, T, T, T
9	9	3	0.45	T, V, T, T, X
9	9	4	0.2	T, T, T, T, X
11	4	3	0.2	T, V, T, T, X
11	6	6	0.2	V, T, T, T, T
11	8	3	0.45	T, V, X, T, X
11	9	1	0.2	T, V, T, X, X
11	9	2	0.45	T, T, X, X, X
13	4	3	0.45	T, T, T, T, T
13	8	2	0.2	T, T, T, X, X
13	8	3	0.45	T, V, T, T, T
15	5	0	0.45	T, T, T, T, X
15	5	1	0.45	T, T, T, T, X
15	6	3	0.45	T, T, X, X, T

[a] Letters correspond to experimental pressures of 0.2, 0.5, 1.0, 1.5 and 2.0×10^5 Pa (0.2, 0.5, 1.0, 1.5 and 2.0 bar), respectively.

3. Results and discussion

3.1. Filtration behaviour

In the absence of membrane fouling and/or cake clogging a plot of t/V versus V in dead-end filtration should lead a straight line with a slope that is proportional to the specific cake resistance. In experiments over a wide range of conditions, all our t/V versus V plots obtained during the initial cake formation step, were found to be linear suggesting that the performance of the filtration system employed in this study is dominated by the cake resistance.

Fig. 2 shows plots of specific cake resistance, measured by the steady-state method, as a function of pressure, at various pHs. The magnitudes of the specific resistance values are in agreement with other workers [32] and [33], but higher than those of Nakanishi et al. [3] and McCarthy et al. [28]. This is probably due to variations in the types of dried yeast employed in each study as well as differences in the various cell washing regimens used. It should be noted also that differences in specific resistance values can occur depending on whether this parameter is defined in terms of a dry cell mass or a wet cell mass. In general, the specific resistance based on a dry cell mass will be larger than its wet cell equivalent.

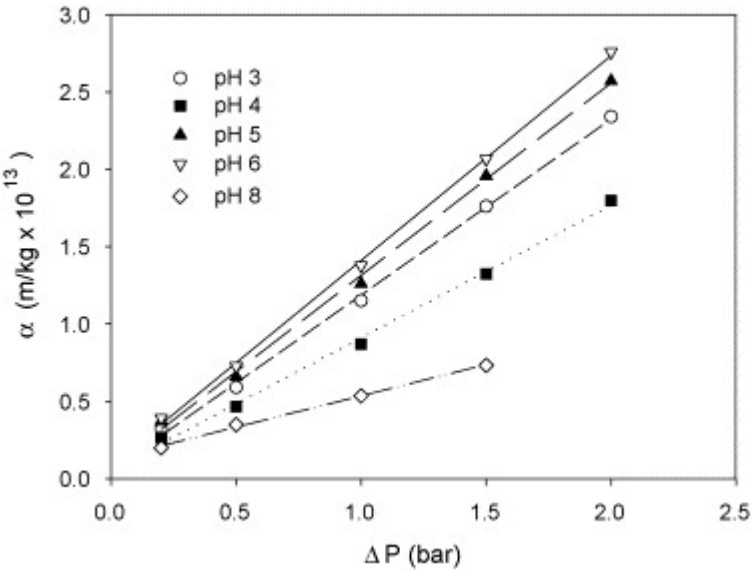

Figure 2: Effect of pH and pressure on the specific cake resistance for a yeast concentration of 5g/L and a pore size of 0.45µm

In Fig. 2, the dependence of specific resistance on pressure is shown to be linear in agreement with other workers [6], [7] and [8] and there is a strong and complex dependence on pH of both the specific resistance at a given pressure and of the cake compressibility, where the latter is proportional to the slope of the α versus ΔP plot [7] and [34].

Fig. 3 shows the dependence of specific resistance on pH at two salt concentrations and various pressures. The apparent complexity of the behaviour means that a conventional non-linear regression approach to developing a correlation of specific resistance will prove problematic because in that

approach some functional relationship between specific resistance and the various parameters affecting it must be assumed. This relationship is likely to be quite complicated and unwieldy in form.

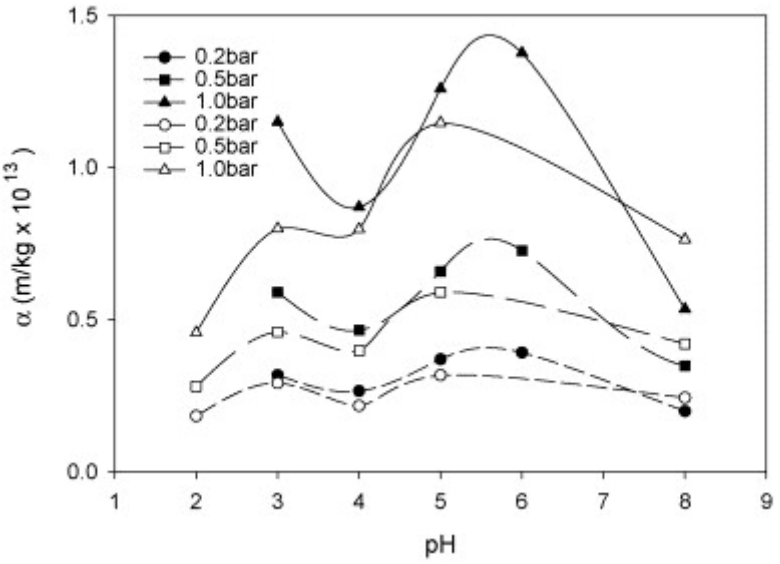

Figure 3: Effect of salt concentration on the specific resistance at various pHs and pressures for a yeast concentration of 5 g/L and a membrane pore size of 0.45 µm. Closed symbols: salt concentration = 2 g/L. Open symbols: salt concentration = 6 g/L.

As mentioned in Section 1, there is now tentative evidence that the specific cake resistance may show a dependence on suspension concentration. Mota et al. [19] found that the specific resistance increased with increasing concentration of yeast cells, while Zaidi and Kumar [20] found a similar effect with silica suspensions. In the work of Mota et al. [19], the specific resistance approximately doubled as the dry weight cell concentration increased from about 4 to 40 g/L, at pressures of 40 and 80 kPa. Zaidi and Kumar [20] found that the specific resistance of silica suspensions increased by a factor of approximately three as the concentration increased from about 3 to 28 g/L. These results were obtained at pressures of 135, 270 and 405 kPa. However, using linear regression, we found that the slopes of plots of specific resistance versus yeast concentration were insignificantly different from zero at the 95% confidence level and can conclude that concentration has no apparent effect on specific resistance.

The results outlined in this section have shown that the specific cake resistance is a complex parameter and is dependent on a number of different variables. The correlation of specific resistance data is difficult, therefore, and new approaches to developing regression equations are required. The following sections outline our results obtained by implementing an approach based on artificial neural networks.

3.2. Determination of optimum network architecture

The network architecture refers to the number of layers in the network and the number of neurons in each layer. It has been shown previously that just one hidden layer is generally sufficient to model most data sets in membrane separation processes [23]. Training of the network is performed by updating the networks weights over a number of epochs, or iterations, until the MSE in the validation data set begins

to increase. This use of the validation set avoids the problem of overtraining [35]. Optimisation of the network architecture, with the aim of minimising the MSE for the training data, was performed via a trial and error procedure. The effect of the number of hidden neurons on the MSE is shown in Fig. 4 (MSE for nine neurons = 9.85×10^{-8}) and, on that basis, a 5-9-1, fully connected architecture was chosen.

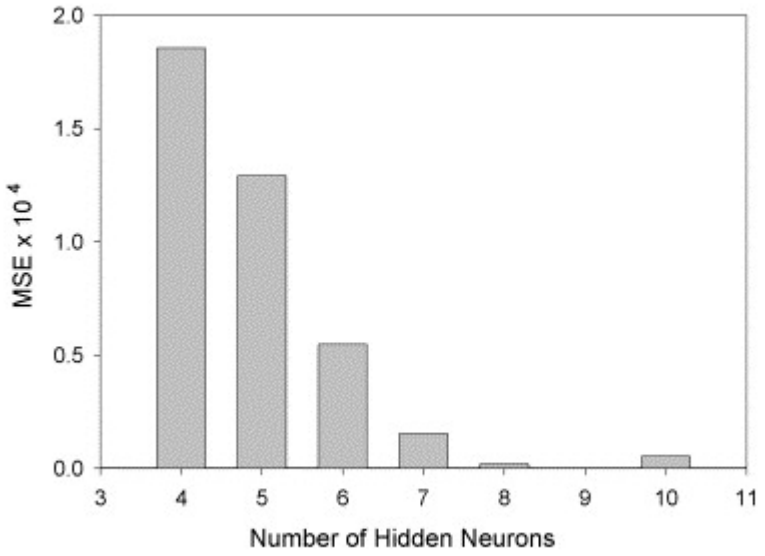

Figure 4: Optimisation of network architecture

3.3. Fit of ANN to specific resistance data

Fig. 1 shows the fit of a 5-9-1 network to the full set of specific resistance data, including those used in training, validation and testing. For the vast majority of the data, the network is able to predict the specific resistance to within 10%. Therefore, the neural network approach offers a potential alternative to more traditional regression techniques for correlating specific resistance behaviour, especially when factors in addition to pressure are included in the analysis. In combination with conventional filtration theory, e.g. Eq. (3), the neural network could be used to form a hybrid model that calculates filtration performance over a wide range of suspension and process conditions.

3.4. Fit of ANN to flux data

While the focus of this paper has been to develop an ANN to predict the specific resistance from which process characteristics can be calculated using Eq. (3), we have also investigated the possibility of using an ANN to predict the filtrate flux data directly. The advantage of this approach is not so much its applicability to dead-end filtration, since the experimental set-up is somewhat artificial and does not reflect the true batch nature of industrial filtration process, but because the ANN for predicting steady fluxes is easily extended to crossflow systems where specific resistance measurements are very difficult to obtain [36]. Fig. 5 shows the fit of a 5-9-1 network obtained in the experiments described above. Exactly the same training, testing and validation sets as for the specific resistance network were used, although a superior fit may have been obtained if a new training set had been chosen specifically for the

flux data. As can be seen, the ANN for the flux correlates the data well and could form the basis of an ANN applied to predicting steady-state fluxes in crossflow systems once additional inputs such as crossflow velocity, and module geometry are included.

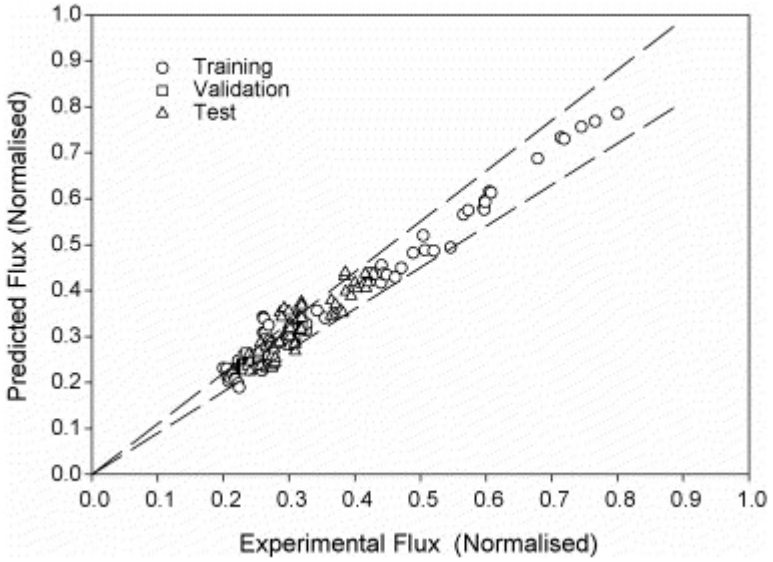

Figure 5: Fit of 5-9-1 network applied to flux data. Dashed lines denote ± 10% variation from the y=x line

3.5. Interpreting the network weights

In this paper, we have shown that an artificial neural network can be used to correlate dead-end specific resistance and flux data. However, previous researchers have shown that the network weights corresponding to an apparently best fitting network are not unique [37]. Indeed, two networks with identical architecture, trained with the same data, may model that data with very similar accuracy and yet the final network weights obtained will almost certainly not be the same. The initial values of the weights (which are initialized here to random values between −0.1 and +0.1) have a strong effect on the final weights obtained for the trained network. This is because the initial weight vector determines the network starting point on the error hyper-space [26]. There is a tendency, when training, for the network to move into the closest local minimum to the starting point on the error surface, rather than to obtain the global minimum. The number of hidden neurons is directly proportional to the number of local minima in the error surface, and therefore adding more hidden neurons to the network will increase the risk of the network becoming trapped in a local minimum.

This variability in the weights obtained when training a network has implications for interpreting the network weights. Traditionally, ANNs have been looked on as ‘black-box’ models, where an accurate description of the process is not required, relying merely on the ability of neural networks to approximately calculate the outputs of a system from knowledge of its inputs [22]. However, some attempts have been made to assess the network connection weights in order to quantitatively derive some cause–effect information. The equation used by Chellam [23], developed by Garson [38], can be written

(6) $$v = \frac{\sum_{j=1}^{n_h}\left[\left(w_{vj} \Big/ \sum_{k=1}^{n_v} w_{kj}\right) O_j\right]}{\sum_{i=1}^{n_v}\left[\sum_{j=1}^{n_h}\left[\left(w_{vj} \Big/ \sum_{k=1}^{n_v} w_{kj}\right) O_j\right]\right]}$$

where $\underline{v}$ represents the relative effect of the input variable, $\underline{v}$, on the output, n_v the number of input variables, n_h the number of neurons in the hidden layer, $\underline{w_{kj}}$ represents the absolute value of the weight from the kth input to the jth neuron and O_j represents the absolute value of the weight from the jth neuron. However, since the network weights are variable, depending on the initial weights used in the training process, the computed effects of input parameters will also be variable. To investigate this phenomenon, we trained the 5-9-1 specific resistance and flux networks over a series of 20 runs with random initial weights in each case. While the effects of the inputs on the output were found to vary, this variation was small as shown in Fig. 6 and Fig. 7 suggesting that the variability of network weights does not make their interpretation impossible.

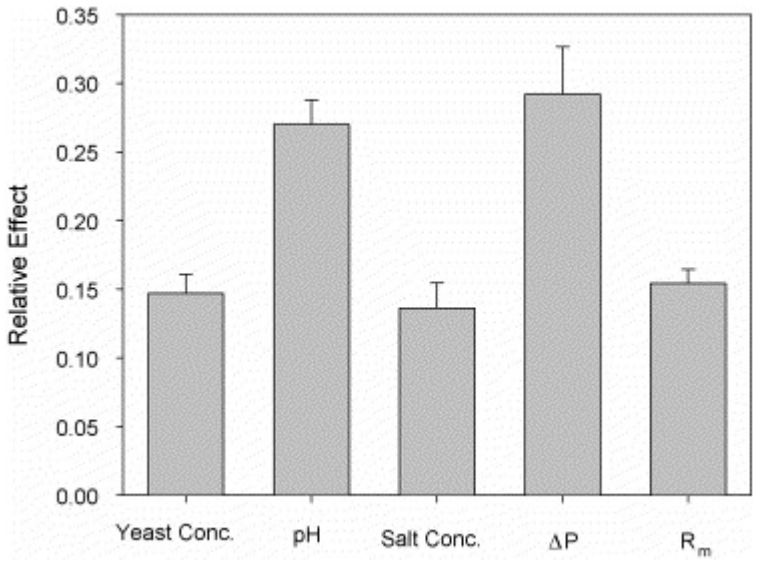

Figure 6: The (mean) relative effect of input parameters on the specific cake resistance. The error bars denote the standard error over 20 runs.

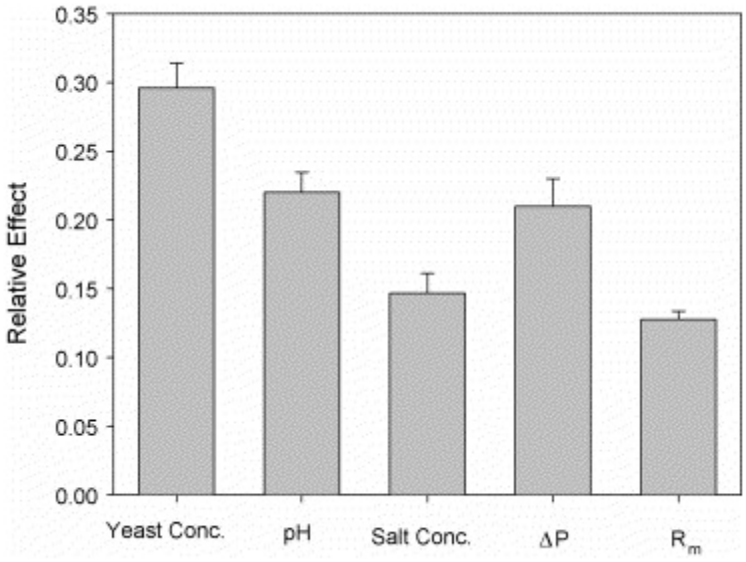

Figure 7: The mean relative effect of input parameters on the steady-state flux. The error bars denote the standard error over 20 runs.

From Fig. 6, we see that the main parameters affecting the specific resistance are the pressure and the pH, as would have been expected from Fig. 2 and Fig. 3. The effects of the other parameters are lower but not insignificant. It is important to note, however, that this approach is only semi-quantitative and a non-zero value for the relative effect of a parameter does not imply a cause–effect relationship but simply shows that the experimental output was different for various values of a given input. This variation may have been due to normal experimental scatter rather than representing a true relationship. Fig. 7 gives the relative effects of the input parameters on the flux. The effect of yeast concentration on the flux is large, as would be expected from Eq. (3) where the concentration appears explicitly in the mechanistic filtration theory. The other parameters that have the most effect are the pressure and the pH. This approach of calculating the relative effects of various input parameters on the system output would be most useful in complex systems where the underlying physics was not well understood and it was desired to identify key process parameters. However, its semi-quantitative nature means that it will only serve as a guide that may aid in reducing the amount of experimentation required but will not lead to a true physical understanding of the process.

4. Conclusions

This study focused on the correlation of specific cake resistance and flux data in dead-end filtration of yeast suspensions using artificial neural networks. The results obtained show that excellent agreement between experimental data and predicted values could be achieved over wide ranges of pressure, membrane resistance, yeast concentration, and suspension pH and ionic strength. The approach is easily extended to include the many other factors that affect the specific resistance. The neural network for the steady-state flux would be easy to extend to encompass crossflow filtration by the addition of parameters such as the crossflow velocity and module configuration. The network weights were interpreted using the equation suggested by Garson [38] to evaluate the relative effect of the input parameters on the specific cake resistance and the steady-state flux. This is an area that is worthy of further study as it is very desirable to be able to extract meaning from the weight matrix of neural networks.

Acknowledgements

We thank Dr. Michael Parkinson for his assistance with statistics for this paper, and the National Institute for Cellular Biotechnology for funding this work.

References

[1] L.J. Zeman and A.L. Zydney, Microfiltration and Ultrafiltration, Marcel Dekker, New York (1996).

[2] A. Rushton, A.A.S. Ward and R.G. Holdich, Solid–Liquid Filtration and Separation Technology, VCH, Weinheim, New York (1996).

[3] K. Nakanishi, T. Tadokoro and R. Matsuno, On the specific resistance of cakes of microorganisms, *Chem. Eng. Commun.* **62** (1987), pp. 187–201.

[4] T. Oolman and T.-C. Liu, Filtration properties of mycelial mocrobial broths, *Biotechnol. Prog.* **7** (1991), pp. 534–539.

[5] Y. Shimizu, K.-I. Shimodera and A. Watanabe, Cross-flow microfiltration of bacterial cells, *J. Ferment. Bioeng.* **76** (1993), pp. 493–500.

[6] T. Tanaka, T.-S. Tsuneyoshi, W. Kitazawa and K. Nakanishi, Characteristics in crossflow filtration using yeast suspensions, *Sep. Sci. Technol.* **32** (1997), pp. 1885–1898.

[7] A.A. McCarthy, D.G. O'Shea, N.T. Murray, P.K. Walsh and G. Foley, Effect of cell morphology on dead-end filtration of the dimorphic yeast *Kluyveromyces marxianus* Var. *marxianus* NRRLy2415, *Biotechnol. Prog.* **14** (1998), pp. 279–285.

[8] A.A. McCarthy, P.K. Walsh and G. Foley, Characterising the packing and dead-end filter cake compressibility of the polymorphic yeast *Kluyveromyces Marxianus* Var. *marxianus* NRRLy2415, *J. Membr. Sci.* **198** (2002), pp. 87–94.

[9] S. Shirato and S. Esumi, Filtration of the cultured broth of *Streptomyces griseus*, *J. Ferment. Technol.* **41** (1963), pp. 87–92.

[10] K. Ohmori and C.E. Glatz, Effects of pH and ionic strength on microfiltration of *C. Glutamicum*, *J. Membr. Sci.* **153** (1999), pp. 23–32.

[11] K. Ohmori, K. Hoshida and E. Iritani, Interactions between cells, proteins and salts in microfiltration of *Corynebacterium glutamicum* slurry, *J. Chem. Eng. Jpn.* **37** (2004), pp. 1497–1503.

[12] P.H. Hodgson, G.L. Leslie, R.P. Schneider, A.G. Fane, C.J.D. Fell and K.C. Marshall, Cake resistance and solute rejection in bacterial microfiltration—the role of the extracellular cell matrix, *J. Membr. Sci.* **79** (1993), pp. 35–53.

[13] K. Ohmori and C.E. Glatz, Effect of carbon source on microfiltration of *Corynebacterium glutamicum*, *J. Membr. Sci.* **171** (2000), pp. 263–271.

[14] K. Ohmori and E. Iritani, Effect of addition of amino acids on microfiltration behavior of a microorganism slurry, *J. Chem. Technol. Biotechnol.* **79** (2004), pp. 1169–1173.

[15] Y. Okamoto, K. Ohmori and C.E. Glatz, Harvest time effects on membrane cake resistance of *Escherichia coli* broth, *J. Membr. Sci.* **190** (2001), pp. 93–106.

[16] M. Meireles, E. Lavoute and P. Bacchin, Filtration of a bacterial fermentation broth: harvest conditions effects on cake hydraulic resistance, *Bioprocess Biosys. Eng.* **25** (2003), pp. 309–314.

[17] T. Tanaka, R. Kamimura, R. Fujiwara and K. Nakanishi, Crossflow filtration of yeast cultivated in molasses, *Biotechnol. Bioeng.* **43** (1994), pp. 1094–1101.

[18] K. Ohmori and E. Iritani, Ultrafiltration behaviour of *Corynebacterium glutamicum* slurry with and without bovine serum albumin, *J. Chem. Eng. Jpn.* **37** (2004), pp. 842–849.

[19] M. Mota, J.A. Teixeira, A. Yelshin, Dependence of *Saccharomyces cerevisiae* filtration through membrane on yeast concentration. In: Proceedings of the Ninth World Filtration Congress, New Orleans, 2004.

[20] S.K. Zaidi and A. Kumar, Experimental analysis of a gel layer in dead-end ultrafiltration of a silica suspension, *Desalination* **172** (2005), pp. 107–117.

[21] R.-Q. Fu, T.-W. Xu and Z.-X. Pan, Modelling of the adsorption of bovine serum albumin on porous polyethylene membrane by back-propagation artificial neural network, *J. Membr. Sci.* **251** (2005), pp. 137–144.

[22] E. Piron, E. Latrille and F. René, Application of artificial neural networks for crossflow microfiltration modelling: “black-box” and semi-physical approaches, *Comput. Chem. Eng.* **21** (1997), pp. 1021–1030.

[23] S. Chellam, Artificial neural network model for transient crossflow microfiltration of polydispersed suspensions, *J. Membr. Sci.* **258** (2005), pp. 35–42.

[24] W.R. Bowen, M.G. Jones and H.N.S. Yousef, Prediction of the rate of cross-flow membrane ultrafiltration of colloids—a neural network approach, *Chem. Eng. Sci.* **53** (1998), pp. 3793–3802.

[25] P. Rai, G.C. Majumdar, S. DasGupta and S. De, Modelling the performance of batch ultrafiltration of synthetic fruit juice and mosambi juice using artificial neural network, *J. Food Eng.* **71** (2005), pp. 273–281.

[26] W.R. Bowen, M.G. Jones, J.S. Welfoot and H.N.S. Yousef, Predicting salt rejections at nanofiltration membranes using artificial neural networks, *Desalination* **129** (2000), pp. 147–162.

[27] G.R. Shetty and S. Chellam, Predicting membrane fouling during municipal drinking water nanofiltration using artificial neural networks, *J. Membr. Sci.* **217** (2003), pp. 69–86.

[28] A.A. McCarthy, P. Gilboy, P.K. Walsh and G. Foley, Characterisation of cake compressibility in dead-end microfiltration of microbial suspensions, *Chem. Eng. Commun.* **173** (1999), pp. 79–90.

[29] W.R. Bowen, M.G. Jones and H.N.S. Yousef, Dynamic ultrafiltration of proteins—a neural network approach, *J. Membr. Sci.* **146** (1998), pp. 225–235.

[30] M.A. Razavi, A. Mortazavi and M. Mousavi, Dynamic modeling of milk ultrafiltration by artificial neural network, *J. Membr. Sci.* **220** (2003), pp. 47–58.

[31] S.-I. Amari, N. Murata, K.-R. Müller, M. Finke and H.H. Yang, Asymptotic statistical theory of overtraining and cross-validation, *IEEE Trans. Neural Networks* **8** (1997), pp. 985–996.

[32] A. Rushton and H.E. Khoo, Filtration characteristics of yeast, *J. Appl. Chem. Biotechnol.* **27** (1977), pp. 99–109.

[33] E. Piron, F. Rene and E. Latrille, A crossflow-microfiltration model based on integration of the mass transport equation, *J. Membr. Sci.* **108** (1995), pp. 57–70.

[34] A.A. McCarthy, H. Conroy, P.K. Walsh and G. Foley, The effect of pressure on the specific resistance of yeast filter cakes during dead-end filtration in the range 30–500 kPa, *Biotechnol. Techniq.* **12** (1998), pp. 909–912.

[35] H.R. Maier and G.C. Dandy, Neural networks for the prediction and forecasting of water resources variables: a review of modelling issues and applications, *Environ. Modelling Software* **15** (2000), pp. 101–124.

[36] A.A. McCarthy, P.K. Walsh and G. Foley, Experimental techniques for quantifying the cake mass, the cake and membrane resistances and the specific cake resistance during crossflow filtration of microbial suspensions, *J. Membr. Sci.* **201** (2002), pp. 31–45.

[37] B. Curry and P.H. Morgan, Model selection in neural networks: some difficulties, *Eur. J. Oper. Res.* **170** (2006), pp. 567–577.

[38] G.D. Garson, Interpreting neural network connection weights, *AI Expert* **6** (1991), pp. 47–51.

Appendix A.

A.1. Sample calculation of the relative effect of input parameters using the Garson equation

Consider a neural network with two inputs, a single hidden layer with three neurons and a single output. After training of the network, the network weights are found to have the values given in Table 3.

Table 3.

Sample absolute values of network weights in a 2-3-1 neural network

From first input to hidden layer		From second input to hidden layer		From hidden layer to output	
w_{11}	0.517	w_{21}	0.649	O_1	0.981
w_{12}	0.162	w_{22}	0.132	O_2	0.461
w_{13}	0.488	w_{23}	0.458	O_3	0.641

The relative effect of the first input on the network output is given, according to the Garson equation, by the expression:

$$v = \frac{(0.517/0.517+0.649)0.981+(0.162/0.162+0.132)0.461 + (0.488/0.488+0.584)0.641}{X+Y}$$

where

$$X = \left(\frac{0.517}{0.517+0.649}\right)0.981 + \left(\frac{0.162}{0.162+0.132}\right)0.461 + \left(\frac{0.488}{0.488+0.584}\right)0.641$$

and

$$Y = \left(\frac{0.649}{0.517+0.649}\right)0.981 + \left(\frac{0.132}{0.162+0.132}\right)0.461 + \left(\frac{0.584}{0.488+0.584}\right)0.641$$

Thus, the relative effect of the first input works out to be 0.5078.